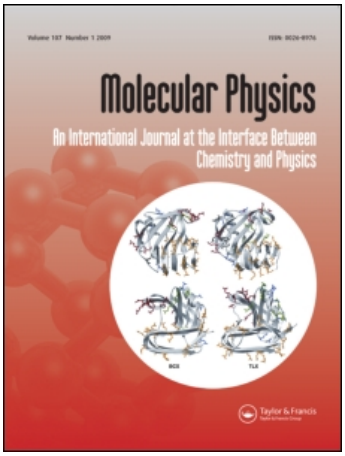
This article was downloaded by: *[Ruhr-universitaet Bochum]*
On: *3 November 2010*
Access details: *Access Details: [subscription number 731929787]*
Publisher *Taylor & Francis*
Informa Ltd Registered in England and Wales Registered Number: 1072954 Registered office: Mortimer House, 37-41 Mortimer Street, London W1T 3JH, UK



Molecular Physics
Publication details, including instructions for authors and subscription information:
http://www.informaworld.com/smpp/title~content=t713395160

Density dependence of electric properties of binary mixtures of inert gases

Antonio Rizzo[a]; Sonia Coriani[b]; Domenico Marchesan[b]; Javier López Cacheiro[c]; Berta Fernández[c]; Christof Hättig[d]
[a] Istituto per i Processi Chimico-Fisici del Consiglio Nazionale delle Ricerche, Area della Ricerca, I-56124 Pisa, Italy [b] Dipartimento di Scienze Chimiche, Università degli studi di Trieste, I-34127 Trieste, Italy [c] Department of Physical Chemistry, Faculty of Chemistry, University of Santiago de Compostela, e-15782 santiago de composa, Spain [d] Forschungszentrum Karlsruhe, Institute of Nanotechnology, D-76021 Karlsruhe, Germany

To cite this Article Rizzo, Antonio , Coriani, Sonia , Marchesan, Domenico , Cacheiro, Javier López , Fernández, Berta and Hättig, Christof(2006) 'Density dependence of electric properties of binary mixtures of inert gases', Molecular Physics, 104: 2, 305 — 318
To link to this Article: DOI: 10.1080/00268970500282133
URL: http://dx.doi.org/10.1080/00268970500282133

PLEASE SCROLL DOWN FOR ARTICLE

Full terms and conditions of use: http://www.informaworld.com/terms-and-conditions-of-access.pdf

This article may be used for research, teaching and private study purposes. Any substantial or systematic reproduction, re-distribution, re-selling, loan or sub-licensing, systematic supply or distribution in any form to anyone is expressly forbidden.

The publisher does not give any warranty express or implied or make any representation that the contents will be complete or accurate or up to date. The accuracy of any instructions, formulae and drug doses should be independently verified with primary sources. The publisher shall not be liable for any loss, actions, claims, proceedings, demand or costs or damages whatsoever or howsoever caused arising directly or indirectly in connection with or arising out of the use of this material.

Molecular Physics, Vol. 104, No. 2, 20 January 2006, 305–318

Taylor & Francis
Taylor & Francis Group

Density dependence of electric properties of binary mixtures of inert gases

ANTONIO RIZZO*†, SONIA CORIANI‡, DOMENICO MARCHESAN‡, JAVIER LÓPEZ CACHEIRO§, BERTA FERNÁNDEZ§ and CHRISTOF HÄTTIG¶

†Istituto per i Processi Chimico-Fisici del Consiglio Nazionale delle Ricerche, Area della Ricerca, via G. Moruzzi 1, loc. S. Cataldo, I-56124 Pisa, Italy
‡Dipartimento di Scienze Chimiche, Università degli studi di Trieste, via L. Giorgieri 1, I-34127 Trieste, Italy
§Department of Physical Chemistry, Faculty of Chemistry, University of Santiago de Compostela, E-15782 Santiago de Compostela, Spain
¶Forschungszentrum Karlsruhe, Institute of Nanotechnology, PO Box 3640, D-76021 Karlsruhe, Germany

(*Received 12 June 2005; in final form 1 August 2005*)

Downloaded By: [Ruhr-universitaet Bochum] At: 14:21 3 November 2010

A computational study of the density dependence of the refractivity and dielectric constants, the electric-field induced second harmonic generation (ESHG) hyperpolarizabilities and of the Kerr constants of binary mixtures of helium, neon and argon is presented. Potentials and interaction properties of the homonuclear A_2 and heteronuclear AB dimers (A, B = He, Ne, Ar) are taken from a previous study [J. López Cacheiro, B. Fernández, D. Marchesan, S. Coriani, C. Hättig, A. Rizzo. *Molec. Phys.*, **102**, 101 (2004)]. Dispersion coefficients for the second virial coefficients allow for the determination of the density dependence at any frequency far from the lowest resonance. Fully quantum mechanical results are presented and a comparison with the corresponding classical estimates is discussed. Deep minima are predicted to occur in the ESHG second virial coefficient curve drawn as a function of the molar fraction of one of the components in binary mixtures of He/Ar and Ne/Ar. This phenomenon, observed over a wide range of temperatures, should be easily verifiable experimentally.

1. Introduction

It is well known that intermolecular forces play a major role in physics, chemistry and biology. The electromagnetic properties of compressed gases are reckoned to yield information about intermolecular forces [1] and in particular rare gases have been the subject of many studies. On the other hand, the *ab initio* determination of intermolecular interaction properties allows the refinement of thermophysical standards [2–4], besides representing an ideal test bed for wave function models and their ability to reproduce response properties of various orders and complexity. The subject of interaction-induced properties has received much attention over the last two decades [5]. From the theoretical point of view their evaluation is a challenge, since, due to the weakness of the interaction, the demands on the basis set and on the electron correlation treatment are high. In previous work, we carried out accurate studies of the interatomic potentials and of various interaction-induced electric properties and second virial coefficients of the helium [6–11], neon [12] and argon [6, 7, 10, 11, 13] homonuclear dimers. Recently, we also presented a study of the interatomic potentials and of the interaction-induced dipole moments, electric dipole polarizabilities, and first and second electric dipole hyperpolarizabilities of the heteronuclear dimers of the same rare gases [14]. In all cases both the potentials and the interaction-induced properties were obtained using size-extensive coupled-cluster methods—mainly CCSD and CCSD(T)—correlation consistent basis sets extended with midbond functions and applying the counterpoise correction of Boys and Bernardi [15] to account for basis set superposition errors.

*Corresponding author. Email: rizzo@ipcf.cnr.it

Molecular Physics
ISSN 0026–8976 print/ISSN 1362–3028 online © 2006 Taylor & Francis
http://www.tandf.co.uk/journals
DOI: 10.1080/00268970500282133

Downloaded By: [Ruhr-universitaet Bochum] At: 14:21 3 November 2010

Following the theory by Buckingham and co-workers [1, 16] for the virial coefficients for mixtures in a compressed gas, here we conclude the investigation on the interaction-induced properties of helium, neon and argon by presenting the second virial coefficients for the dielectric constant and refractivity, the electric second harmonic generation (ESHG) hyperpolarizability and the Kerr constant of binary mixtures.

The second virial coefficients are evaluated using both a classical and a quantum statistical approach over a wide range of temperatures. The ingredients are the interaction-induced properties for the heterodimers presented and discussed in [14], together with those of the homonuclear dimers collected from our previous work [6, 12]. Most of the calculations of virial coefficients for the pure gases were already performed in our previous studies [7, 10, 11], the exception being the fully quantum mechanical estimates of the ESHG hyperpolarizability and Kerr constant second virial coefficients of helium and argon. Nevertheless we have recomputed anew all values for the present study, adopting homogeneous computational conditions across the set of dimers and taking advantage of improved numerical algorithms, which allowed for wider integration intervals and tighter convergence thresholds in the integrations.

Dielectric second virial coefficient measurements in mixtures involving CF_3H–Ar and CFH_3–Ar were presented quite some years ago by Copeland and Cole [17]. Experimentally, these properties are not easy to obtain, as shown in our previous work, where we found revision of the experimental data to be needed [10]. To our knowledge, the second virial coefficients for the binary mixtures of helium, neon and argon gases presented here have not yet been measured, and thus no comparison can be made with experimental data. The aim of our work is thus to predict their magnitude. Considering the methods and basis sets we use, we can expect to get accurate values for these properties that can help in the interpretation of the experimental data.

2. Properties and virials for binary mixtures

Following the lines of the theory given in [1, 16], a chosen (measurable) property of the real gas can be written as a power series of the gas density ρ, i.e. as a virial type expression

$$Q = A_Q + B_Q\rho + C_Q\rho^2 + \cdots \tag{1}$$

with the coefficients A_Q, $B_Q, \ldots,$ defining the first, second, …, virial coefficients. See also [11, 18–21]. Thus, the first term in the expansion corresponds to the perfect gas contribution to the property, whereas the second (third, etc.) is the contribution arising from all interacting pairs (triples, etc.) of particles.

For a mole of an ideal molecular gas—that is, for a system of N_A non-interacting particles (where N_A is Avogadro's number)—one would have

$$Q \equiv A_Q = qN_A, \tag{2}$$

where q denotes the contribution of an individual molecule to the property Q. Within a classical theory, the second virial coefficient B_Q for spherical particles 1 and 2 can be associated with the following quantity [11, 16]

$$B_Q = 4\pi N_A^2 \int \left[\frac{1}{2}q_{12}(R) - \frac{q_1 + q_2}{2}\right] \exp\left[-\frac{V(R)}{k_B T}\right] R^2 \, dR, \tag{3}$$

where k_B is Boltzmann's constant, T is the temperature, R is the distance between the two particles, q_{12} is the property Q for the dimer and $V(R)$ is the interparticle potential.

The generalizations of the above equations for gas mixtures are [1]

$$A_Q = \sum_i x_i A_{Q,i}; \quad B_Q = \sum_{i,j} x_i B_{Q,ij} x_j, \tag{4}$$

where x_i is the mole fraction of the ith component of the mixture. In the specific case of a binary mixture of rare gas atoms, the total density dependence is thus a function of the two-body interactions between atoms of the same chemical species as well as those between different species. The resulting effect can be decomposed as [1]

$$Q = x_1 A_{Q,1} + x_2 A_{Q,2} + \frac{1}{V_m} B_{Q,\mathrm{mix}} + \cdots, \tag{5}$$

$$B_{Q,\mathrm{mix}}(T, x_1) = x_1^2 B_{Q,11}(T) + x_2^2 B_{Q,22}(T) + 2x_1 x_2 B_{Q,12}(T), \tag{6}$$

where $V_m = (x_1 M_1 + x_2 M_2)/\rho_m$ is the molar volume (written in terms of the molecular masses M_1 and M_2 and the density of the mixture ρ_m), $B_{Q,11}$, $B_{Q,22}$ are the second virial coefficients for the homonuclear dimers and $B_{Q,12}$ that of the heteronuclear dimer.

The extensive properties we will look at in the following are the dielectric constant

Downloaded By: [Ruhr-universitaet Bochum] At: 14:21 3 November 2010

(Clausius–Mossotti function) and the molar refractivity, the second electric dipole hyperpolarizability for the ESHG and the molar Kerr constant. We will calculate the second virial coefficients $B_{Q,ii}$ and $B_{Q,ij}$ for each property at various temperatures. Frequency-dependent properties will be written as analytic second-order expansions in the frequency to determine the density dependence over the whole range of frequencies below the first excited state resonance.

The electronic contribution to the interaction property q_{12} is written as

$$\Delta P(R) = P_{12}(S_{1-2}|R) - P_1(S_{1-2}|R) - P_2(S_{1-2}|R), \quad (7)$$

where $P_{12}(S_{1-2}|R)$ is the property of the dimer evaluated in the dimer basis set S_{1-2} at the interatomic distance R and $P_1(S_{1-2}|R)[P_2(S_{1-2}|R)]$ the property of monomer 1(2) evaluated in the dimer basis set at the same geometry. The above expression contains the counterpoise correction proposed by Boys and Bernardi [15] for the basis set superposition error.

It is also convenient to introduce the notation $X[\Delta P(R), V(R), T]$ to denote, in the classical approach, the integral over the internuclear coordinate [22]

$$X[\Delta P(R), V(R), T] = 4\pi \int \Delta P(R) \exp\left[-\frac{V(R)}{k_B T}\right] R^2 \mathrm{d}R. \quad (8)$$

In the following, we will shorten the notation dropping the reference to the interparticle potential $V(R)$ in the arguments of the function X. The fully quantum-mechanical counterpart of the same quantity is [22, 23]

$$X[\Delta P(R), T] = 4\pi\lambda_B^3 \sum_{J=0}^{\infty}(2J+1)\left[1+\frac{(-1)^{J+2I}}{2I+1}\right] \times \left\{\sum_n \exp\left[-\frac{E_{nJ}}{k_B T}\right]\langle\xi_{nJ}(R)|\Delta P(R)|\xi_{nJ}(R)\rangle + \int_0^{\infty} \exp\left[-\frac{\hbar^2 k^2}{2\mu k_B T}\right]\langle\xi_{kJ}(R)|\Delta P(R)|\xi_{kJ}(R)\rangle \frac{\mu}{\hbar^2 k}\mathrm{d}k\right\}, \quad (9)$$

where ξ_{nJ} and ξ_{kJ} are the radial parts of the bound and continuum eigenfunctions of the field-independent Hamiltonian (energies E_{nJ} and E_{kJ}, respectively), labelled by the rotational quantum number J, the vibrational quantum number n and the wave number k. λ_B is the thermal wavelength ($\lambda_B = (\hbar^2/2\mu k_B T)^{1/2}$), μ the reduced mass and I the nuclear spin quantum number. Equation (9), which was originally derived for dielectric second virial coefficients [22, 23] and used for this purpose in [10, 12, 24], can be extended to frequency-dependent and/or higher-order properties as the ESHG hyperpolarizability and Kerr constant second virial coefficients under some approximations (frequency of the external field(s) large compared to the vibrational transition frequency) which are fairly acceptable for most of the frequencies of interest for the weakly bound van der Waals complexes of rare gas dimers [25].

2.1. *Dielectric and refractivity virial coefficients*

The dielectric virial coefficient B_ϵ is the second-order coefficient in the series expansion of the Clausius–Mossotti function [1, 16–18, 20, 26]

$$\frac{\epsilon-1}{\epsilon+2} = A_\epsilon\rho + B_\epsilon\rho^2 + C_\epsilon\rho^3\cdots, \quad (10)$$

where ϵ is the relative dielectric permittivity. Then

$$A_\epsilon = \frac{N_A}{3\epsilon_0}\left(\alpha_{ave} + \frac{\mu^2}{3k_B T}\right) \quad (11)$$

with the last term in parentheses averaging to zero for dynamical fields in the optical range. α_{ave} is the average electric dipole polarizability, μ is the permanent electric dipole moment and ϵ_0 is the vacuum permittivity. In equation (3) then, taking into account that the formulae given are valid for the special case of heteronuclear atomic dimers (and thus dipole moments, first dipole hyperpolarizabilities and anisotropies of the electric dipole polarizabilities of the monomers vanish), the dimer and monomer properties become

$$q_{12} = \frac{1}{3\epsilon_0}\left(\alpha_{ave,12} + \frac{\mu_{12}^2}{3k_B T}\right), \quad (12)$$

$$q_1 = \frac{1}{3\epsilon_0}\alpha_1. \quad (13)$$

Employing a power expansion, see [27], where the interaction-induced average electric dipole polarizability at the frequency ω, $\Delta\alpha_{ave}(-\omega;\omega)$, is written as

$$\Delta\alpha_{ave}(-\omega;\omega) \approx \Delta\alpha_{ave}(0) + \omega^2\Delta S_{ave}(-4); \quad (14)$$

with $\Delta\alpha_{ave}(0)$ as the static average electric dipole polarizability and $\Delta S_{ave}(-4)$ as the interaction-induced

Cauchy moment, we obtain

$$B_\epsilon = B_R^{(0),\alpha} + B_\epsilon^{\mu^2} \tag{15}$$

$$B_R = B_R^{(0),\alpha} + \omega^2 B_R^{(2),\alpha} \tag{16}$$

and

$$B_R^{(0),\alpha} = \frac{N_A^2}{6\pi\epsilon_0} X[\Delta\alpha_{ave}(0), T], \tag{17}$$

$$B_\epsilon^{\mu^2} = \frac{N_A^2}{18\epsilon_0 k_B T} X[(\Delta\mu)^2, T], \tag{18}$$

$$B_R^{(2),\alpha} = \frac{N_A^2}{6\epsilon_0} X[\Delta S_{ave}(-4), T]. \tag{19}$$

Note once again that the contribution involving the interaction-induced dipole moment does not enter the expression of B_R, equation (16), as we are considering dynamical fields in the optical range.

2.2. *Electric field induced second harmonic generation (ESHG)*

The quantity measured in an ESHG experiment, when light is polarized parallel to an applied static field, is in the limit of very low pressure [28, 29]

$$\chi_\parallel^e(\omega, T) = \left\{\gamma_\parallel(-2\omega;\omega,\omega,0) + \frac{1}{3k_B T}\mu\beta_\parallel(-2\omega;\omega,\omega)\right\} \tag{20}$$

with the direction of the permanent dipole moment μ defining the z molecular axis (note that $\chi_\parallel^e(\omega, T)$ as defined throughout this paper is a factor of six larger than introduced for instance in [28, 29]). Expressions for $\gamma_\parallel$ and $\beta_\parallel$ can be found in [28].

The density dependence of $\chi_\parallel^e$ is written as, see equation (1)

$$\chi_\parallel^e(\omega, T, \rho) = \chi_\parallel^e(\omega, T) + B_\parallel(\omega, T)\rho + \cdots, \tag{21}$$

where $\chi_\parallel^e(\omega, T)$ is given by equation (20). We then have in reference to equation (3)

$$q_{12} = \frac{1}{N_A}\left\{\gamma_{\parallel,12}(-2\omega;\omega,\omega,0) + \frac{1}{3k_B T}\mu_{12}\beta_{\parallel,12}(-2\omega;\omega,\omega)\right\}, \tag{22}$$

$$q_1 = \frac{1}{N_A}\left\{\gamma_{\parallel,1}(-2\omega;\omega,\omega,0)\right\} \tag{23}$$

and introducing the frequency dispersion of the interaction-induced properties through the expansions of [30, 31]

$$\Delta\gamma_\parallel(-2\omega;\omega,\omega,0) \approx \Delta\gamma_\parallel(0) + \omega^2\Delta D_{ESHG}^{\gamma}(2), \tag{24}$$

$$\Delta\beta_\parallel(-2\omega;\omega,\omega) \approx \Delta\beta_\parallel(0) + \omega^2\Delta D_{ESHG}^{\beta}(2), \tag{25}$$

yields expressions for the ESHG second virial coefficient

$$B_\parallel = B_\parallel^{(0)} + \omega^2 B_\parallel^{(2)}, \tag{26}$$

$$B_\parallel^{(0)} = B_\parallel^{(0),\gamma} + B_\parallel^{(0),\mu\beta}, \tag{27}$$

$$B_\parallel^{(2)} = B_\parallel^{(2),\gamma} + B_\parallel^{(2),\mu\beta}, \tag{28}$$

where

$$B_\parallel^{(0),\gamma} = \frac{N_A}{8\pi\epsilon_0} X[\Delta\gamma_\parallel(0), T], \tag{29}$$

$$B_\parallel^{(0),\mu\beta} = \frac{N_A}{24\pi\epsilon_0 k_B T} X[\Delta\mu\Delta\beta_\parallel(0), T], \tag{30}$$

$$B_\parallel^{(2),\gamma} = \frac{N_A}{8\pi\epsilon_0} X[\Delta D_{ESHG}^{\gamma}(2), T], \tag{31}$$

$$B_\parallel^{(2),\mu\beta} = \frac{N_A}{24\pi\epsilon_0 k_B T} X[\Delta\mu\Delta D_{ESHG}^{\beta}(2), T]. \tag{32}$$

2.3. *dc-Kerr effect*

In the dc-Kerr experiment, the quantity of interest is the so-called Kerr constant ${}_mK$ [32], which can be expanded in a power series in the density as [32, 33]

$${}_mK = A_K + B_K\rho + C_K\rho^2 + \cdots, \tag{33}$$

where [34–36]

$$A_K = \frac{N_A}{81\epsilon_0}\left\{\gamma_K(\omega) + \frac{2}{3k_B T}\mu\beta_K(\omega) + \frac{1}{5k_B T}\alpha_{ani}(\omega)\alpha_{ani}(0) + \frac{1}{5(k_B T)^2}\mu^2\alpha_{ani}(\omega)\right\}. \tag{34}$$

Downloaded By: [Ruhr-universitaet Bochum] At: 14:21 3 November 2010

Downloaded By: [Ruhr-universitaet Bochum] At: 14:21 3 November 2010

The dc-Kerr first and second dipole hyperpolarizabilities $\beta_K(\omega)$ and $\gamma_K(\omega)$ are defined in [28]. We have in this case

$$q_{12} = \frac{1}{81\epsilon_0}\left\{\gamma_{K,12}(\omega) + \frac{2}{3k_BT}\mu_{12}\beta_{K,12}(\omega) + \frac{1}{5k_BT}\alpha_{ani,12}(\omega)\alpha_{ani,12}(0) + \frac{1}{5(k_BT)^2}\mu_{12}^2\alpha_{ani,12}(\omega)\right\}, \quad (35)$$

$$q_1 = \frac{1}{81\epsilon_0}\gamma_{K,1}(\omega), \quad (36)$$

which, expanding the frequency dispersion [27, 30, 31] for the interaction-induced electric dipole polarizability anisotropy $\Delta\alpha_{ani}(-\omega;\omega)$ and for the dc-Kerr hyperpolarizabilities $\Delta\beta_K(-\omega;\omega,0)$ and $\Delta\gamma_K(-\omega;\omega,0,0)$ as

$$\Delta\alpha_{ani}(-\omega;\omega) \approx \Delta\alpha_{ani}(0) + \omega^2\Delta S_{ani}(-4), \quad (37)$$

$$\Delta\beta_K(-\omega;\omega,0) \approx \Delta\beta_\parallel(0) + \omega^2\Delta D_K^\beta(2), \quad (38)$$

$$\Delta\gamma_K(-\omega;\omega,0,0) \approx \Delta\gamma_\parallel(0) + \omega^2\Delta D_K^\gamma(2), \quad (39)$$

yields the expression of the second dc-Kerr virial coefficient as

$$B_K = B_K^{(0)} + \omega^2 B_K^{(2)}, \quad (40)$$

$$B_K^{(0)} = B_K^{(0),\gamma} + B_K^{(0),\mu\beta} + B_K^{(0),\alpha^2} + B_K^{(0),\mu^2\alpha}, \quad (41)$$

$$B_K^{(2)} = B_K^{(2),\gamma} + B_K^{(2),\mu\beta} + B_K^{(2),\alpha^2} + B_K^{(2),\mu^2\alpha} \quad (42)$$

with

$$B_K^{(0),\gamma} = \frac{N_A^2}{162\epsilon_0}X[\Delta\gamma_\parallel(0), T], \quad (43)$$

$$B_K^{(0),\mu\beta} = \frac{N_A^2}{243\epsilon_0 k_BT}X[\Delta\mu\Delta\beta_\parallel(0), T], \quad (44)$$

$$B_K^{(0),\alpha^2} = \frac{N_A^2}{910\epsilon_0 k_BT}X[[\Delta\alpha_{ani}(0)]^2, T], \quad (45)$$

$$B_K^{(0),\mu^2\alpha} = \frac{2\pi N_A^2}{910\epsilon_0(k_BT)^2}X[(\Delta\mu)^2\Delta\alpha_{ani}(0), T], \quad (46)$$

$$B_K^{(2),\gamma} = \frac{N_A^2}{81\epsilon_0}X[\Delta D_K^\gamma(2), T], \quad (47)$$

$$B_K^{(2),\mu\beta} = \frac{2N_A^2}{243\epsilon_0 k_BT}[\Delta\mu\Delta D_K^\beta(2), T], \quad (48)$$

$$B_K^{(2),\alpha^2} = \frac{N_A^2}{910\epsilon_0 k_BT}X[\Delta\alpha_{ani}(0)\Delta S_{ani}(-4), T], \quad (49)$$

$$B_K^{(2),\mu^2\alpha} = \frac{N_A^2}{910\epsilon_0(k_BT)^2}X[(\Delta\mu)^2\Delta S_{ani}(-4), T]. \quad (50)$$

Note that we have assumed Kleinman symmetry [37] for all homonuclear dimers and thus $\Delta D_K^\gamma(2) \approx 3\Delta D_{ESHG}^\gamma(2)$ and $B_K^{(2),\gamma} \approx (8\pi N_A/81)B_\parallel^{(2),\gamma}$. The validity of this assumption is confirmed by the comparison of our current results for the neon dimer with those published in [12], where we employed directly the $\Delta D_K^\gamma(2)$ expansion coefficients.

3. Computational details

All virial coefficients were computed employing the program KORG [38]. The general integral $X[\Delta Q(R), T]$ was determined both performing a classical integration, see equation (8), and by employing a fully quantum-statistical approach, see equation (9) [10, 12].

The integration of the one-dimensional Schrödinger equation was performed for He_2 for an internuclear distance R going from 2.0 to 200.0 au, for Ne_2 from 3.0 to 300.0 au and for Ar_2 from 4.5 to 200.0 au. In all three cases a step size of 0.0004 au was used. Integration over k (the wave number) was carried out from $k = 0.5$ to 300.0 au for He_2 and Ar_2, and from $k = 0.4$ to 300.0 au for Ne_2. The technique employed to ensure convergence is described in [10, 12].

For He_2 the results presented here are those obtained with the FCI/d-aug-cc-pV5Z-321 extrapolated potential and properties, see [6, 7]. Both potential and properties were analytically fitted in the form and with the parameters given in [6, 7].

For Ne_2 the potential is the CCSD(T)/d-aug-cc-pV5Z proposed by Halkier *et al.* [39] whereas the properties are the CCSD/d-aug-cc-pVQZ-33211 ones given in [12]. Both potential and properties were analytically fitted in the form and with the parameters given in [12].

For Ar_2 the CCSD(T)/d-aug-cc-pV5Z-33211 potential was taken from [40], see also [13]. The properties—static values calculated at the CCSD/d-aug-cc-pVQZ level and frequency power expansion coefficients obtained at the CCSD/d-aug-cc-pVTZ level—were taken from [13]. The potential and the zero-order contributions to the frequency dependent terms had been already analytically fitted in the form and with the parameters given in [6, 7]. For the frequency power expansion coefficients (whose fits are not available in the literature) $\Delta S_{ave}(-4)$, $\Delta S_{ani}(-4)$ and $\Delta D_{ESHG}^\gamma(2)$, the data published in [13] (see table 3, p. 2876) were fitted to appropriate functional forms in the present work.

Downloaded By: [Ruhr-universitaet Bochum] At: 14:21 3 November 2010

For the HeNe and HeAr dimers, integration of the one-dimensional Schrödinger equation over the internuclear distance R was performed in the interval between 2.5 and 200.0 au, with a step size of 0.0004 au. For NeAr the lower integration limit was set equal to 4.5 au. For this heterodimer we also obtained all virial coefficients repeating all calculations by taking the lower integration limit down to $R = 3.0$ au, and the results we obtained cannot be distinguished from those obtained with the lower limit at $R = 4.5$ au within the accuracy displayed in our tables. Integration in the continuum over k went from $k = 0.5$ to 300.0 au. The functional forms used in the integration for the interatomic potential and the interaction-induced dipole moments, polarizabilities and hyperpolarizabilities are the fitting functions of the CCSD(T)/aug-cc-pV6Z-33211 potentials and the CCSD/d-aug-cc-pVQZ-33211 interaction-induced properties presented in [14].

For all systems the sum over rotational states J in the fully quantum mechanical calculations, see equation (9), goes up to $J = 500$. In some cases (namely for the integrals involving the frequency power expansion coefficients, equations (31) and (47), in the heaviest dimer, Ar_2), this was not sufficient to reach an adequate level of convergence. This problem has been encountered and discussed already in [10], where it was observed that for high angular momenta J the contribution to the dielectric second virial coefficient was found to decrease approximately as $b \times J^{-c}$, with b and c depending on the temperature. The same functional form fits nicely the high-J contribution also for the other quantum integrals introduced in section 2, and this long-range extrapolation was employed to estimate the quantum mechanical values for $B_{\parallel}^{(2),\gamma}$ in the argon dimer. Since for this dimer we assumed Kleinman symmetry [37], see above, this reflects also in the way we obtained the quantum mechanical values for $B_{\mathrm{K}}^{(2),\gamma}$.

Masses were taken as those tabulated for the most abundant isotopes: 4.002 603 24 amu for He, 19.992 4356 amu for Ne and 39.962 3837 amu for Ar, taken from [41]. The conversion factors used are (i) for B_R and B_ϵ $1\,\mathrm{au} = a_0^6\,\mathrm{mol}^{-2} = 2.19587 \times 10^{-50}\,\mathrm{cm}^6\,\mathrm{mol}^{-2}$; (ii) for $B_\parallel$ $1\,\mathrm{au} = e^4 a_0^{13} m_e^3 \hbar^{-6}\,\mathrm{mol}^{-1} = 9.23988 \times 10^{-96}$ SI units ($\mathrm{C}^4\,m^7\,\mathrm{J}^{-3}\,\mathrm{mol}^{-1}$); (iii) for B_{K} $1\,\mathrm{au} = e^2 a_0^{12} m_e^2 \hbar^{-4}\,\mathrm{mol}^{-2} = 8.30439 \times 10^{-86}$ SI units ($\mathrm{V}^{-2}\,m^8\,\mathrm{mol}^{-2}$), see [41].

4. Results and discussion

Table 1 collects the quantum-statistical results for the various contributions to the dielectric and refractivity virial coefficients in equations (15) and (16) of both the homonuclear and heteronuclear dimers given at a selection of temperatures in a range from the dissociation temperature (estimated by our potential curves at 11 K for He_2, 37 K for Ne_2, 143 K for Ar_2, 20 K for HeNe, 30 K for HeAr and 66 K for NeAr) to 420 K. The corresponding results for the various contributions to the ESHG and Kerr effect, see equations (26) and (40), are given in tables 2 and 3, respectively. (Results for more temperatures in this

Table 1. Contributions to the dielectric and refractivity virial coefficients, see equations (15) to (19). Units are $\mathrm{cm}^6\,\mathrm{mol}^{-2}$. See text.

T/K	$B_R^{(0),\alpha}$	$B_R^{(2),\alpha}$	$B_\epsilon^{\mu^2}$	B_ϵ
He_2				
35	−0.0115	−0.1071		−0.0115
95	−0.0244	−0.1493		−0.0244
170	−0.0367	−0.1919		−0.0367
250	−0.0474	−0.2282		−0.0474
330	−0.0565	−0.2587		−0.0565
420	−0.0656	−0.2883		−0.0656
Ne_2				
35	−0.0600	−0.6307		−0.0600
95	−0.0511	−0.4645		−0.0511
170	−0.0654	−0.4987		−0.0654
250	−0.0807	−0.5497		−0.0807
330	−0.0948	−0.5983		−0.0948
420	−0.1092	−0.6480		−0.1092
Ar_2				
170	1.6717	6.2680		1.6717
250	1.4743	5.8908		1.4743
330	1.3617	5.4583		1.3617
420	1.2718	4.9888		1.2718
HeNe				
35	−0.0234	−0.2385	0.0006	−0.0228
95	−0.0359	−0.2727	0.0001	−0.0358
170	−0.0501	−0.3258	0.0001	−0.0501
250	−0.0629	−0.3736	0.0001	−0.0628
330	−0.0739	−0.4142	0.0001	−0.0738
420	−0.0849	−0.4537	0.0001	−0.0848
HeAr				
35	−0.1681	−3.7251	0.2203	0.0523
95	−0.1788	−3.2053	0.0921	−0.0866
170	−0.2251	−3.4980	0.0993	−0.1258
250	−0.2703	−3.8347	0.1088	−0.1615
330	−0.3102	−4.1351	0.1133	−0.1969
420	−0.3501	−4.4314	0.1154	−0.2346
NeAr				
95	−0.1042	−3.4084	0.2765	0.1723
170	−0.1194	−3.0392	0.1904	0.0710
250	−0.1539	−3.1164	0.1673	0.0134
330	−0.1890	−3.2770	0.1586	−0.0304
420	−0.2263	−3.4756	0.1542	−0.0720

Table 2. Contributions to the ESHG virial coefficients, see equations (26) to (32). Units are $C^4\,m^7\,J^{-3}\,mol^{-1} \times 10^{-n}$ and the exponent n is given in parentheses in the heading for each system.

T/K	$B_{\parallel}^{(0),\gamma}$	$B_{\parallel}^{(0),\mu\beta}$	$B_{\parallel}^{(0)}$	$B_{\parallel}^{(2),\gamma}$	$B_{\parallel}^{(2),\mu\beta}$	$B_{\parallel}^{(2)}$
He_2 ($n=69$)						
35	−2.1482		−2.1482	−9.1689		−9.1689
95	−2.5665		−2.5665	−10.3409		−10.3409
170	−3.0175		−3.0175	−11.7532		−11.7532
250	−3.3900		−3.3900	−12.9234		−12.9234
330	−3.6913		−3.6913	−13.8644		−13.8644
420	−3.9739		−3.9739	−14.7403		−14.7403
Ne_2 ($n=68$)						
35	−1.0488		−1.0488	−5.6209		−5.6209
95	−0.7030		−0.7030	−3.7009		−3.7009
170	−0.7112		−0.7112	−3.5991		−3.5991
250	−0.7545		−0.7545	−3.6982		−3.6982
330	−0.7995		−0.7995	−3.8254		−3.8254
420	−0.8466		−0.8466	−3.9656		−3.9656
Ar_2 ($n=67$)						
170	0.15757		0.15757	3.5310		3.5310
250	0.30931		0.30931	6.0605		6.0605
330	0.34459		0.34459	6.9358		6.9358
420	0.34516		0.34516	7.3227		7.3227
HeNe ($n=69$)						
35	−4.8041	0.0901	−4.7140	−25.0978	0.4108	−24.6871
95	−4.8607	0.0384	−4.8223	−24.0867	0.1728	−23.9139
170	−5.3700	0.0244	−5.3457	−25.6478	0.1091	−25.5387
250	−5.8429	0.0175	−5.8254	−27.2273	0.0780	−27.1493
330	−6.2380	0.0134	−6.2246	−28.5655	0.0591	−28.5065
420	−6.6129	0.0102	−6.6027	−29.8349	0.0444	−29.7905
HeAr ($n=67$)						
35	−1.1388	0.3125	−0.8263	−11.3627	2.2213	−9.1414
95	−0.9268	0.1575	−0.7692	−9.1050	0.9780	−8.1270
170	−0.9403	0.1204	−0.8199	−9.0696	0.7246	−8.3450
250	−0.9776	0.1039	−0.8737	−9.2975	0.6201	−8.6774
330	−1.0145	0.0949	−0.9196	−9.5462	0.5619	−8.9843
420	−1.0518	0.0884	−0.9634	−9.8059	0.5190	−9.2869
NeAr ($n=67$)						
95	−0.9354	0.2470	−0.6884	−9.4359	1.5011	−7.9348
170	−0.7938	0.1587	−0.6351	−7.8831	0.9298	−6.9533
250	−0.7724	0.1297	−0.6427	−7.5290	0.7386	−6.7904
330	−0.7775	0.1156	−0.6619	−7.4588	0.6442	−6.8145
420	−0.7918	0.1061	−0.6856	−7.4840	0.5804	−6.9036

Downloaded By: [Ruhr-universitaet Bochum] At: 14:21 3 November 2010

range, both classical and quantum statistical, are available for the interested reader upon request.)

Differences between quantum-statistical and classical results can be discussed with reference to figures 1–3, for dielectric and refractivity, ESHG and Kerr, respectively. In the figures the percentage deviation between quantum and classical results is plotted as a function of the temperature, for all but a very few, essentially negligible, contributions, as for example $B_R^{\mu^2}$ for the mixed HeNe dimer.

The extent to which fully quantum mechanical and classical results come close as the temperature increases is on one side a measure of the importance of quantum effects on the virial coefficients and on the other an indication of the accuracy of the integration procedures: extension of the mesh of integration points, completeness of the summation over the rotational quantum number J, importance of the choice of the interval of integration in the continuum index k (both the lowest and the highest thresholds), proper account

Table 3. Contribution to the Kerr second virial coefficients, see equations (40) to (50). Units are $V^{-2}\,m^8\,mol^{-2} \times 10^{-n}$ and the exponent n is given in parentheses in the heading for each system.

T/K	$B_K^{(0),\gamma}$	$B_K^{(0),\alpha^2}$	$B_K^{(0),\mu\beta}$	$B_K^{(0),\mu^2\alpha}$	$B_K^{(0)}$	$B_K^{(2),\gamma}$	$B_K^{(2),\alpha^2}$	$B_K^{(2),\mu\beta}$	$B_K^{(2),\mu^2\alpha}$	$B_K^{(2)}$
He_2 ($n=36$)										
35	−1.8038	21.0491			19.2453	−15.3980	41.1759			25.7779
95	−2.1550	6.7958			4.6408	−17.3663	14.6191			−2.7472
170	−2.5338	4.5393			2.0055	−19.7380	9.3060			−10.4320
250	−2.8465	3.4466			0.6001	−21.7033	6.8226			−14.8807
330	−3.0995	2.8043			−0.2952	−23.2835	5.4138			−17.8697
420	−3.3368	2.3262			−1.0106	−24.7546	4.4077			−20.3469
Ne_2 ($n=35$)										
35	−0.8807	32.7551			31.8744	−9.4396	63.4465			54.0069
95	−0.5903	8.9755			8.3852	−6.2152	17.3401			11.1249
170	−0.5972	4.8061			4.2089	−6.0444	9.2035			3.1591
250	−0.6335	3.2562			2.6227	−6.2106	6.1861			−0.0245
330	−0.6714	2.4797			1.8083	−6.4242	4.6794			−1.7448
420	−0.7109	1.9647			1.2538	−6.6598	3.6838			−2.9760
Ar_2 ($n=34$)										
170	0.1347	110.8155			110.9501	2.9649	541.5806			544.5456
250	0.2620	67.0641			67.3261	5.0889	327.4706			332.5595
330	0.2914	48.4153			48.7066	5.8239	236.0461			241.8700
420	0.2916	37.1046			37.3962	6.1488	180.5712			186.7200
HeNe ($n=35$)										
35	−0.4034	7.7053	0.0151	0.0098	7.3269	−9.1137	15.4042	0.2726	0.0132	6.5764
95	−0.4082	2.6127	0.0064	0.0004	2.2115	−8.7215	5.0923	0.1142	0.0006	−3.5145
170	−0.4509	1.4806	0.0041	0.0001	1.0338	−9.2407	2.8319	0.0717	0.0001	−6.3371
250	−0.4905	1.0286	0.0029	0.0000	0.5410	−9.7716	1.9444	0.0511	0.0001	−7.7761
330	−0.5235	0.7946	0.0022	0.0000	0.2734	−10.2228	1.4893	0.0387	0.0001	−8.6948
420	−0.5547	0.6365	0.0017	0.0001	0.0835	−10.6514	1.1834	0.0292	0.0001	−9.4388
HeAr ($n=34$)										
35	−0.9562	9.4246	0.5247	1.0073	10.0004	−39.0706	27.1328	14.9984	1.1831	4.2438
95	−0.7782	2.8514	0.2646	0.0683	2.4061	−31.2594	8.0147	6.5565	0.0665	−16.6218
170	−0.7896	1.5576	0.2022	0.0220	0.9922	−31.0963	4.2564	4.8953	0.0124	−21.9323
250	−0.8209	1.0635	0.1745	0.0118	0.4289	−31.8431	2.8384	4.2060	0.0009	−24.7978
330	−0.8518	0.8130	0.1594	0.0085	0.1290	−32.6659	2.1282	3.8191	−0.0035	−26.7221
420	−0.8832	0.6457	0.1485	0.0073	−0.0818	−33.5264	1.6594	3.5317	−0.0058	−28.3411
NeAr ($n=34$)										
95	−0.7854	12.3003	0.4147	0.4883	12.4179	−33.1142	37.8216	10.2050	1.1001	16.0125
170	−0.6666	6.0781	0.2666	0.1950	5.8731	−27.6111	18.6024	6.3332	0.4061	−2.2694
250	−0.6486	3.9932	0.2178	0.1194	3.6818	−26.3235	12.1317	5.0355	0.2337	−8.9226
330	−0.6528	2.9944	0.1941	0.0871	2.6228	−26.0392	9.0332	4.3943	0.1624	−12.4494
420	−0.6649	2.3485	0.1783	0.0674	1.9293	−26.0899	7.0340	3.9597	0.1202	−14.9760

Downloaded By: [Ruhr-universitaet Bochum] At: 14:21 3 November 2010

of the quasi-bound resonances appearing for all but the lightest dimer in given intervals of rotational numbers, see [10]. All these variables have been discussed in some detail in [10], and the choices made and precaution taken in the present study should let us confidently assume that both the fully quantum and the semi-classical estimates for the virial coefficients are fairly accurate. On the other hand, it is also reasonable to assume that differences exceeding a fraction of a percent in the two sets of results at the upper extreme of the temperature interval (420 K) might be fully ascribed to numerical inaccuracies, as it is highly unlikely that quantum effects might be of higher relevance at such temperatures.

As can be seen in the figures, in most instances the percentage differences between quantum and semi-classical contributions to the second virial coefficients settle to less than 1% at temperatures reasonably

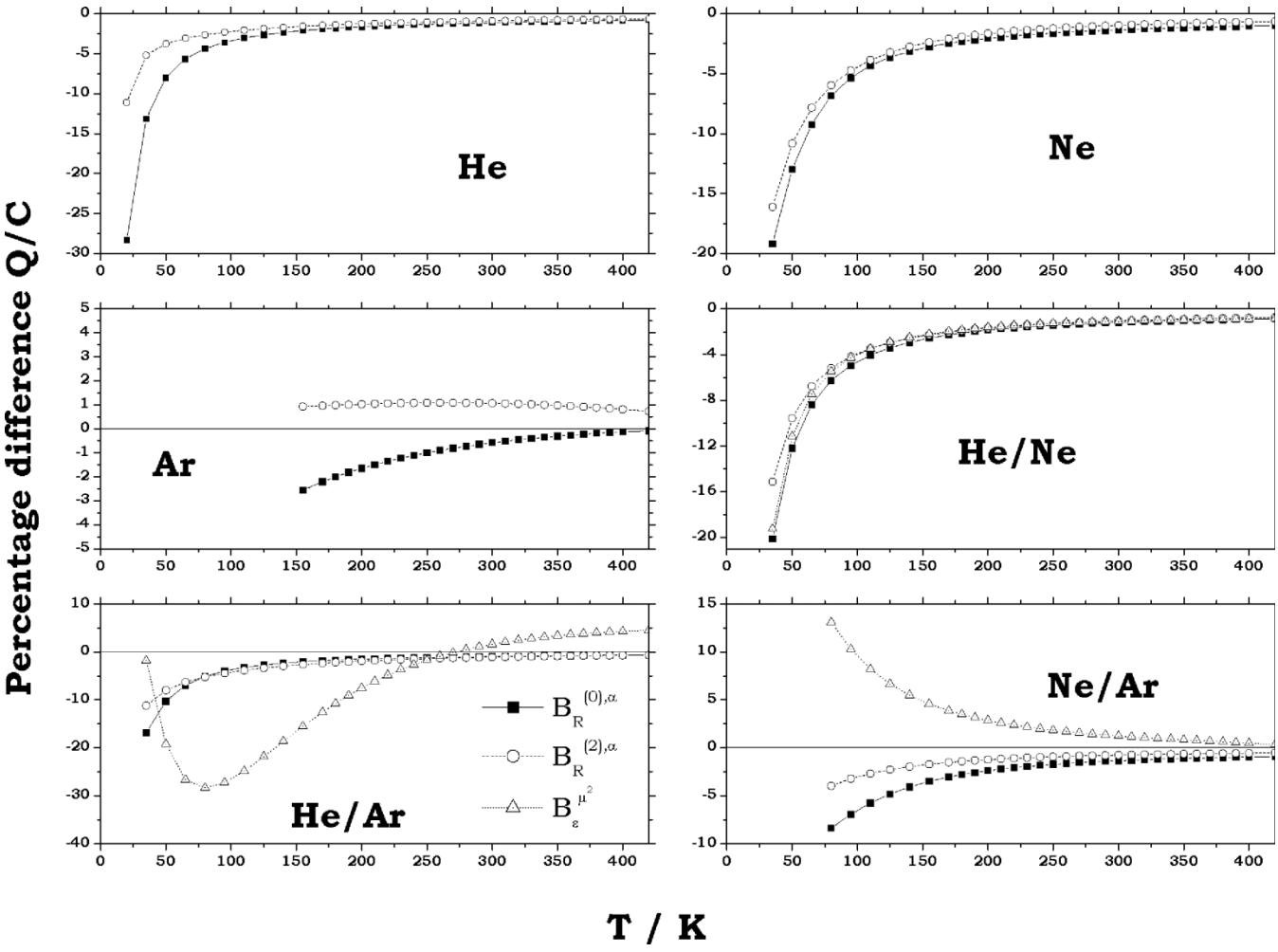


Figure 1. Percentage difference between classical and quantum results for the dielectric and refractivity virial coefficients. The percentage difference for $B_{\epsilon}^{\mu^2}$ of He/Ne dimer is not reported since it results from a comparison of very small numbers, see table 1, and thus is affected by large numerical instabilities.

Downloaded By: [Ruhr-universitaet Bochum] At: 14:21 3 November 2010

below the upper limit of the graphs. In the worst instances, percentage differences never exceed 3–4% at 420 K, and these occur always for contributions intrinsically small if not negligible, as the $B_R^{\mu^2}$ contribution to the dielectric second virial coefficient of the HeAr dimer, the $B_{\parallel}^{(0),\mu\beta}$ and $B_{\parallel}^{(2),\mu\beta}$ contributions to the ESHG second virial coefficient of some mixed dimers, or where apparently the convergence in the summation over the rotational quantum number J is slower, as for $B_{\mathrm{K}}^{(0),\alpha^2}$ of HeNe and HeAr and $B_{\mathrm{K}}^{(2),\alpha^2}$ for the lightest mixed dimer.

Quantum effects are important (taking as a measure the extent to which the percentage difference between the fully quantum and the classical result exceeds 5%) below 70 K for helium, as already observed elsewhere [10, 24], while for neon this is already the case below $\approx$100 K. For argon quantum effects are negligible for the dielectric/refractivity virial coefficient, again see also [10], but not for the hyperpolarizability contributions to the ESHG and Kerr constant second virial coefficients, where percentage differences larger than 5% are still observable at room temperature. The mixed dimers exhibit sizeable quantum effects at temperatures lower than 100 to 150 K, depending on the property and the dimer.

Turning our attention to the quantum results given in the tables, we observe that for the dielectric and the refractivity virial coefficients of the mixed dimers B_{ϵ} is entirely dominated by the polarizability contribution in the case of He/Ne, while the induced electric dipole term plays a non-negligible role and adds with the opposite sign to the polarizability contribution in the mixed He/Ar and Ne/Ar dimers. Frequency dispersion has in general a minor, though not negligible, effect and always strengthens the absolute value of the dielectric

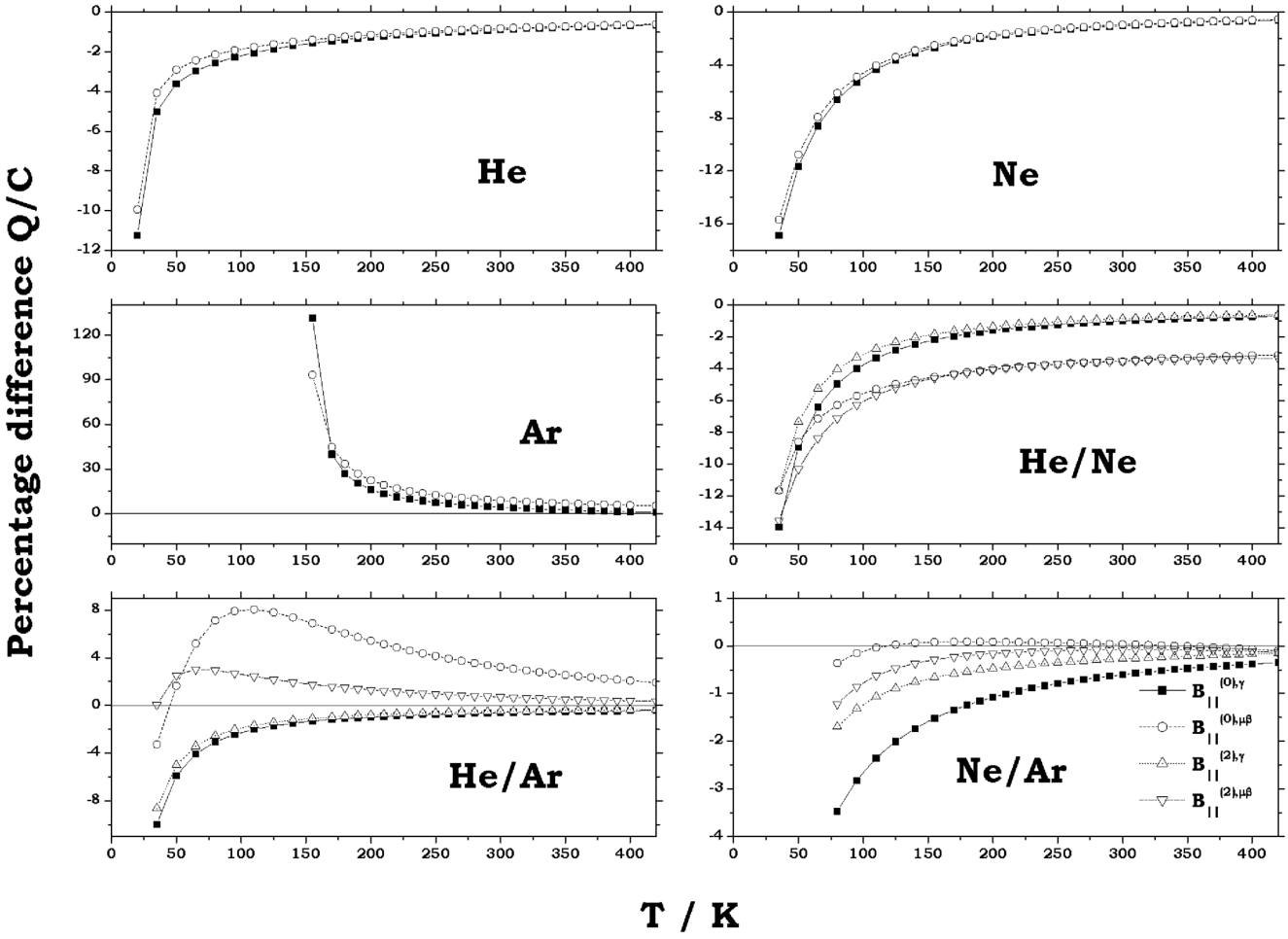


Figure 2. Percentage difference between classical and quantum results for the ESHG virial coefficients.

second virial. The dielectric virial coefficients are of comparable magnitude for He_2, Ne_2 and HeNe. They are about one order of magnitude larger for HeAr and NeAr, whereas the argon dimer exhibits dielectric virial coefficients of opposite sign and one order of magnitude larger than those of HeAr and NeAr.

For the ESHG second virial coefficients we observe that the contributions of $B_{\|}^{\mu\beta}$ are smaller than those of $B_{\|}^{\gamma}$, of opposite sign and getting smaller, as expected, with increasing temperature. Their importance increases in the heavier heteronuclear dimers HeAr and NeAr. In general it is expected that the contributions involving tensorial properties of ungerade symmetry as induced dipole moments or first electric dipole hyperpolarizabilities become more important the larger the differences are in the electronic structure of the two monomers in the van der Waals complex.

Finally, as far as the Kerr constant second virial coefficient is concerned, the $B_{\mathrm{K}}^{\mu^2\alpha}$ term is always rather negligible, the higher the temperature. The $B_{\mathrm{K}}^{\mu\beta}$ contribution is instead of importance, even greater than its size would let us predict, since the two major terms (B_{K}^{γ} and $B_{\mathrm{K}}^{\alpha^2}$) are always of opposite sign, and in delicate balance as the temperature varies. The relationships between these two major contributions to the second virial coefficient of the Kerr constant of helium, neon and argon were discussed in previous communications [7, 12, 13].

To conclude the discussion, we show in figures 4–6 the refractivity, ESHG second electric dipole hyperpolarizability and the Kerr constant second virial coefficients, respectively, as a function of the molar fraction of one of the two components for all three possible mixtures and the set of temperatures employed in tables 1 to 3. The second virial coefficients were computed for a wavelength of 632.8 nm.

The refractivity second virial coefficient of the mixture changes almost linearly as the molar fraction of helium increases, in the He/Ne mixture, cf. equation (4). A minimum, moving with increasing

Downloaded By: [Ruhr-universitaet Bochum] At: 14:21 3 November 2010

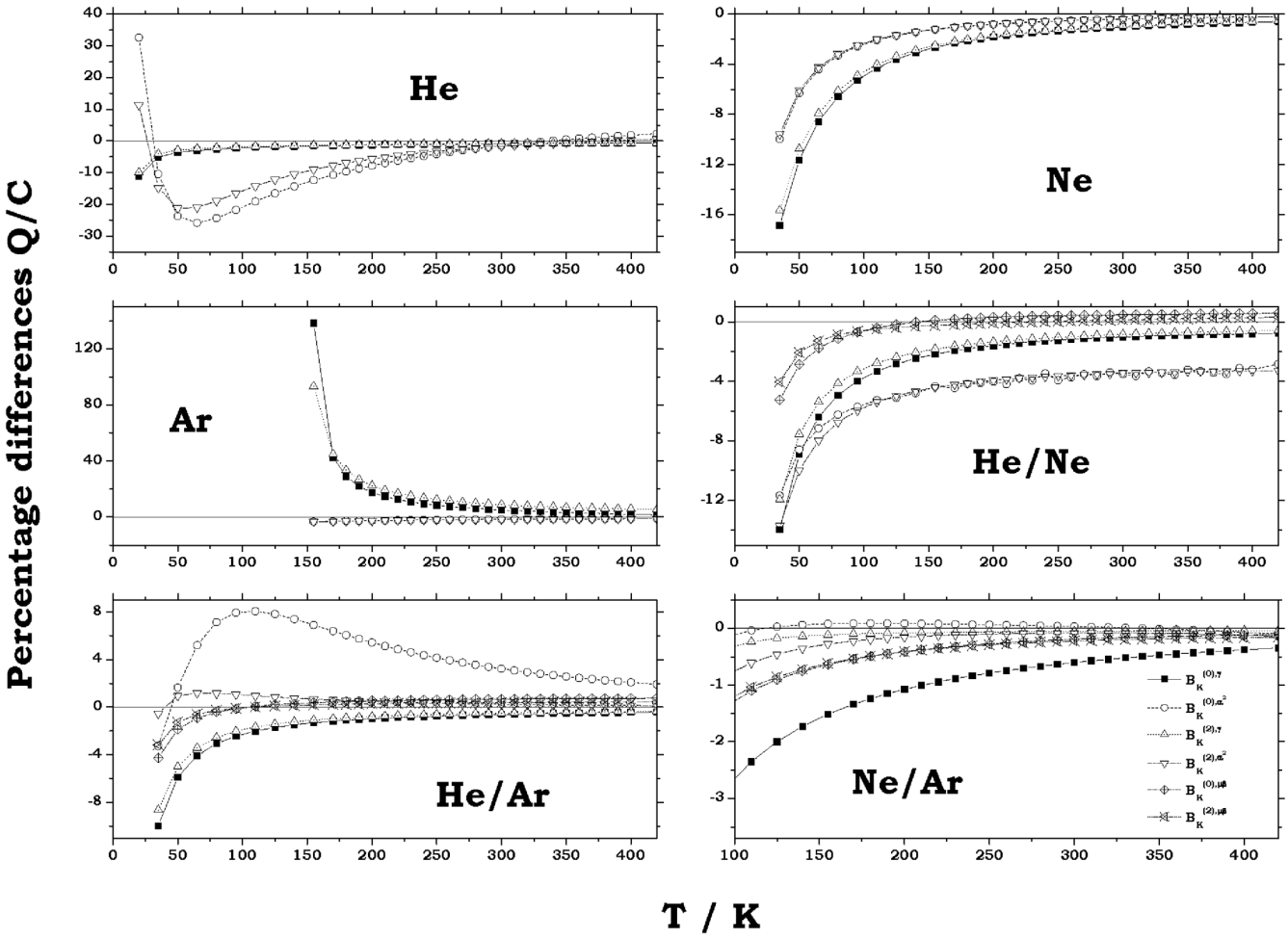


Figure 3. Percentage difference between classical and quantum results for the Kerr virial coefficients.

Downloaded By: [Ruhr-universitaet Bochum] At: 14:21 3 November 2010

temperature to smaller helium molar fractions, is observed instead for the He/Ar. The same minimum appears but is hardly visible, at high temperature for the Ne/Ar mixture.

The ESHG second virial coefficient, see figure 5, for both He/Ar and Ne/Ar mixtures varies noticeably with the change in the composition of the mixture. A deep minimum of around -4.5×10^{-68} SI units (He/Ar) and -4×10^{-68} SI units (Ne/Ar)—cf. the values for the pure gases both in figure 5 and in table 2—arises for a molar fraction of argon around 0.35–0.5, somehow getting deeper (He/Ar) or shallower (Ne/Ar) slowly as the temperature increases. Again, the He/Ne mixtures exhibit a smoothly varying second virial coefficient, albeit with big variations between 35 and 95 K.

The condition for an extremum in the mixture virial coefficients is easily determined from equation (6): for a minimum, it has to be $B_{Q,11}(T) \geq B_{Q,12}(T)$ and $B_{Q,22}(T) \geq B_{Q,12}(T)$, while reverse inequalities must be fulfilled for a maximum. It would be interesting to verify experimentally the occurrence of the pronounced minimum in the ESHG second virial coefficient in the He/Ar or Ne/Ar mixtures. This might experimentally be easier than measuring accurately ratios of virial coefficients, a procedure employed e.g. by Donley and Shelton [42, 43].

The Kerr constant virial coefficient, figure 6, changes by almost three orders of magnitude in the two mixtures involving argon, and by one to two orders of magnitude in the He/Ne mixture. The behaviour as the composition of the mixture changes is smooth. The decrease in the virial coefficient as a small fraction of the lighter component is mixed to the heavier pure component is noticeable.

To conclude, it is appropriate to mention that the accuracy of the second virial coefficients presented in this work depends on several factors. These are both related to the *ab initio* approaches employed in the calculation of the pair potentials and of the interaction electric properties (basis set completeness and extent

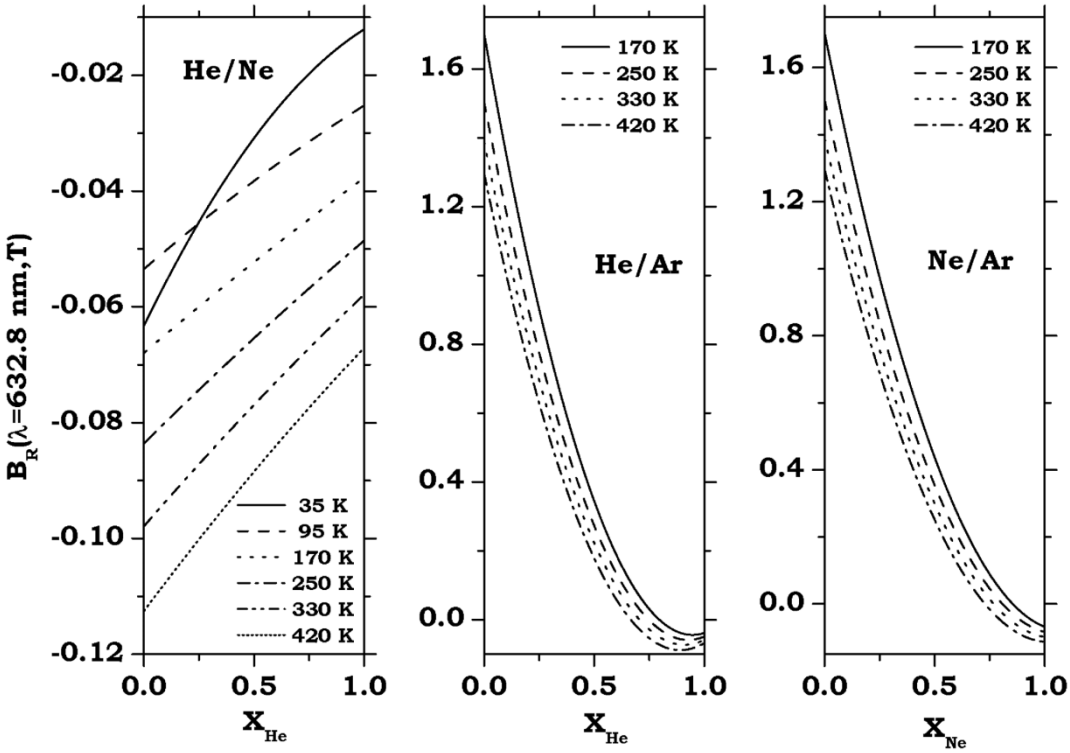


Figure 4. The refractivity second virial coefficient of binary mixtures of helium, neon and argon, at $\lambda = 632.8$ nm, as a function of the molar fraction of one of the components, computed at different temperatures. Units are $cm^6\,mol^{-2}$.

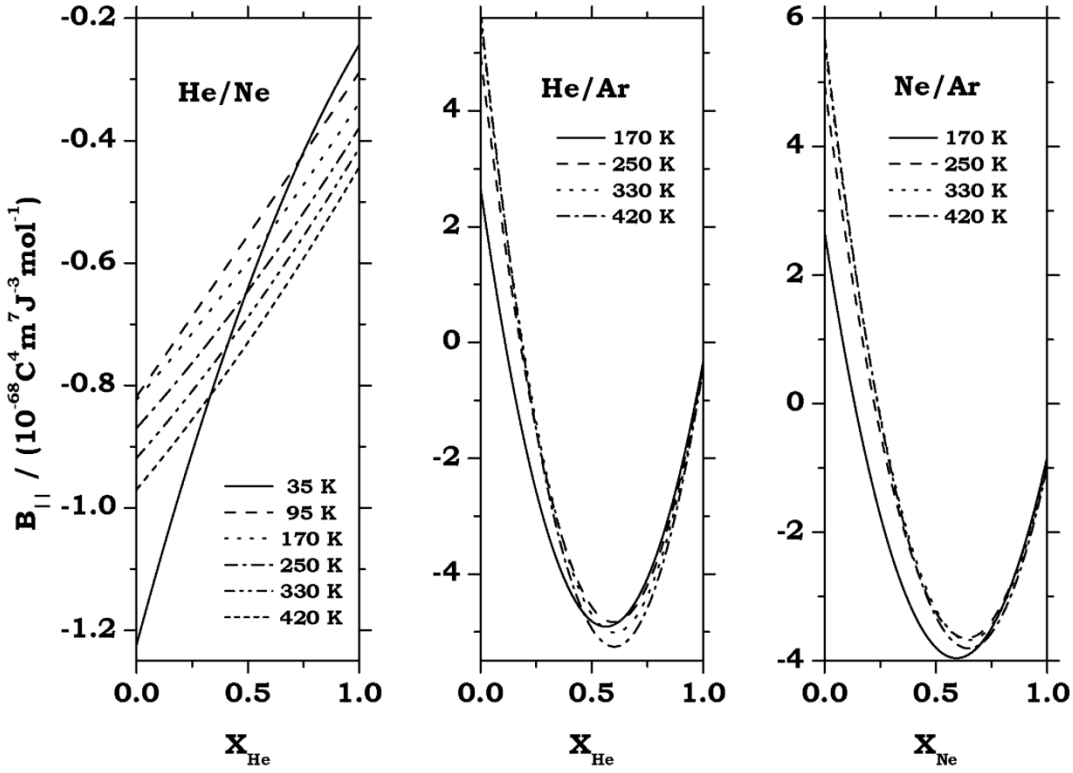


Figure 5. The electric second harmonic generation second virial coefficient of binary mixtures of helium, neon and argon, at $\lambda = 632.8$ nm, as a function of the molar fraction of one of the components, computed at different temperatures.

Downloaded By: [Ruhr-universitaet Bochum] At: 14:21 3 November 2010

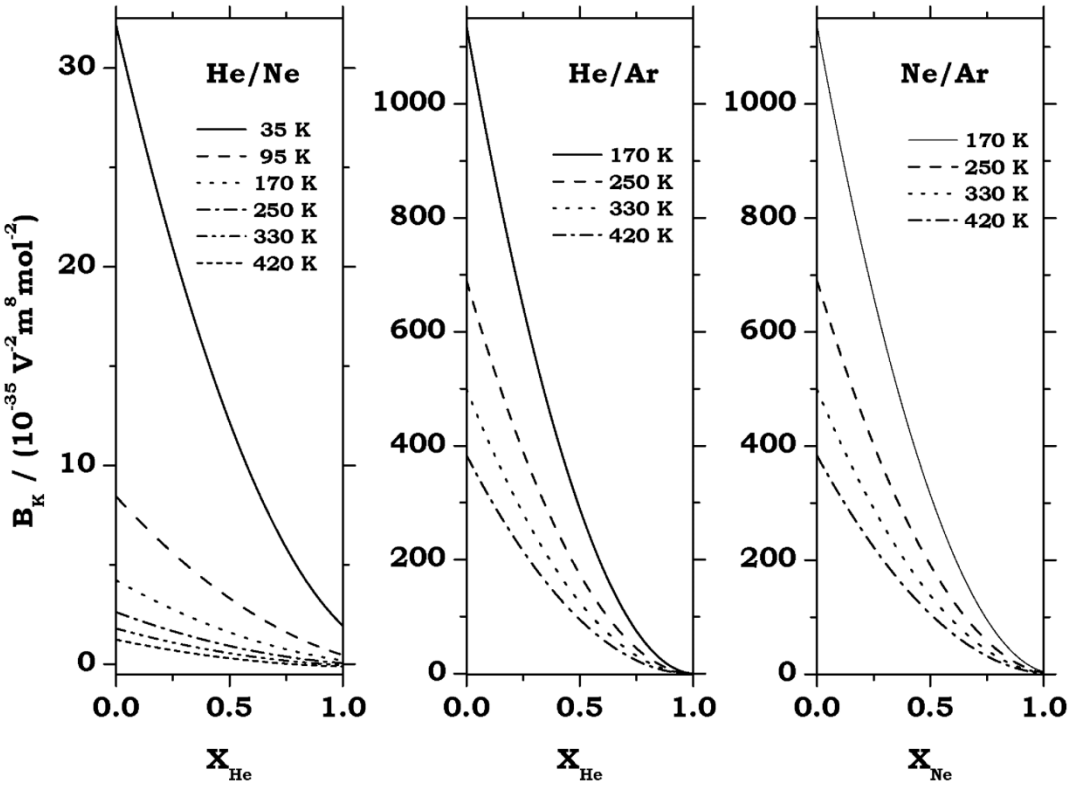


Figure 6. The dc-Kerr second virial coefficient of binary mixtures of helium, neon and argon, at $\lambda = 632.8$ nm, as a function of the molar fraction of one of the components, computed at different temperatures.

Downloaded By: [Ruhr-universitaet Bochum] At: 14:21 3 November 2010

to which the effect of electron correlation is taken into account) and to the control of the fitting and numerical integration procedures employed. The latter are discussed in detail above. As far as the accuracy of the internuclear potentials and interaction electric properties is concerned, it was discussed in our previous studies [6, 10, 12, 13]. Based on basis set convergence analyses (which, due to computational cost, are by necessity limited to very few internuclear distances) and on our experience with coupled cluster models, we concluded that in most cases our interaction properties are accurate to within a few percent. Therefore they are in most cases probably the major sources of uncertainty in the calculation of the properties discussed in this paper. Their level of accuracy is likely to carry over to the second virial coefficients discussed in this work, which should also be considered accurate to a few percent.

5. Summary

We have carried out a computational study of the second virial coefficients for the dielectric and refractivity, ESHG second dipole hyperpolarizability and Kerr constant of mixtures of helium, neon and argon gases. This study completes an analysis of the density dependence of these three rare gases, and their homonuclear and heteronuclear dimers, and it yields reasonably accurate predictions for the density-dependent properties and response of their binary mixtures to the electric optical perturbation.

All contributions arising in the perturbative theoretical approach—essentially due to Buckingham and co-workers [1, 16]—have been computed, both within a semi-classical and a fully quantum mechanical approximation and an assessment of their relative importance has been made. The interaction-induced properties, including interatomic potential curves, are those presented and discussed in [14]. Those of the homonuclear dimers, although already computed in our group in the past [6, 12, 14], were all recomputed to take advantage of the progress in the computational tools made in recent years.

To our knowledge there are (yet) no data in the literature for the noble gas mixtures to compare with. The present calculations are thus the first predictions for the second refractivity, ESHG and Kerr virial coefficients of their binary mixtures. These show that mixed two-body interactions can

lead to remarkable changes in the density dependence of properties. Striking examples are the ESHG second virial coefficients of He/Ar and Ne/Ar mixtures, which exhibit strong effects of the heteroatomic contributions.

Acknowledgements

This work has been supported by the European Research and Training Network NANOQUANT, contract No. MRTN-CT-2003-506842, and by the Spanish Comisión Interministerial de Ciencia y Tecnología and FEDER (BQU2002-02484 project).

References

[1] A.D. Buckingham, R.E. Raab. *Trans. Faraday Soc.*, **54**, 623 (1958).
[2] M.R. Moldover. *J. Res. Natl. Inst. Stand. Technol.*, **103**, 167 (1998).
[3] J.J. Hurly, M.R. Moldover. *J. Res. Natl. Inst. Stand. Technol.*, **105**, 667 (2000).
[4] M.R. Moldover, T.J. Buckley. *Int. J. Thermophys.*, **22**, 859 (2001).
[5] A.J. Stone. *The Theory of Intermolecular Forces*, Oxford University Press, Oxford (1996).
[6] C. Hättig, H. Larsen, J. Olsen, P. Jørgensen, H. Koch, B. Fernández, A. Rizzo. *J. Chem. Phys.*, **111**, 10099 (1999).
[7] H. Koch, C. Hättig, H. Larsen, J. Olsen, P. Jørgensen, B. Fernández, A. Rizzo. *J. Chem. Phys.*, **111**, 10108 (1999).
[8] M. Pecul, A. Rizzo. *Molec. Phys.*, **100**, 447 (2002).
[9] A. Rizzo, K. Ruud, D.M. Bishop. *Molec. Phys.*, **100**, 799 (2002).
[10] A. Rizzo, C. Hättig, B. Fernández, H. Koch. *J. Chem. Phys.*, **117**, 2609 (2002).
[11] D. Marchesan, S. Coriani, A. Rizzo. *Molec. Phys.*, **101**, 1851 (2003).
[12] C. Hättig, J. López Cacheiro, B. Fernández, A. Rizzo. *Molec. Phys.*, **101**, 1983 (2003).
[13] B. Fernández, C. Hättig, H. Koch, A. Rizzo. *J. Chem. Phys.*, **110**, 2872 (1999).
[14] J. López Cacheiro, B. Fernández, D. Marchesan, S. Coriani, C. Hättig, A. Rizzo. *Molec. Phys.*, **102**, 101 (2004).
[15] S.F. Boys, F. Bernardi. *Molec. Phys.*, **19**, 553 (1970).
[16] A. Buckingham, J. Pople. *Faraday Soc. Disc.*, **22**, 17 (1956).
[17] T.G. Copeland, R.H. Cole. *J. Chem. Phys.*, **64**, 1741 (1976).
[18] A. Buckingham, J. Pople. *Trans. Faraday Soc.*, **51**, 1029 (1955).
[19] A.D. Buckingham, J.A. Pople. *Trans. Faraday Soc.*, **51**, 1173 (1955).
[20] A.D. Buckingham, J.A. Pople. *Trans. Faraday Soc.*, **51**, 1179 (1955).
[21] A.D. Buckingham. *Trans. Faraday Soc.*, **52**, 747 (1956).
[22] J.O. Hirschfelder, C.F. Curtiss, R.B. Bird. *Molecular Theory of Gases and Liquids*, John Wiley & Sons, New York (1954).
[23] T.L. Hill. *Statistical Mechanics: Principles and Selected Applications*, Dover Publications, Inc., New York (1987).
[24] R. Moszynski, T.G.A. Heijmen, A. van der Avoird. *Chem. Phys. Lett.*, **247**, 440 (1995).
[25] C. Hättig, R. Moszynski, A. Rizzo. Unpublished results.
[26] C. Joslin, S. Goldman. *Molec. Phys.*, **79**, 1351 (1993).
[27] C. Hättig, O. Christiansen, P. Jørgensen. *J. Chem. Phys.*, **107**, 10592 (1997).
[28] D.P. Shelton, J.E. Rice. *Chem. Rev.*, **94**, 3 (1994).
[29] J.W. Dudley II, J.F. Ward. *J. Chem. Phys.*, **82**, 4673 (1985).
[30] C. Hättig, P. Jørgensen. *Theor. Chim. Acc.*, **100**, 230 (1998).
[31] C. Hättig, P. Jørgensen. *Adv. Quantum Chem.*, **35**, 111 (1999).
[32] A.D. Buckingham, J.A. Pople. *Proc. Roy. Soc.* A, **68**, 905 (1955).
[33] A.D. Buckingham, D.A. Dunmur. *Trans. Faraday Soc.*, **64**, 1776 (1968).
[34] C.J.F. Böttcher, P. Bordewijk. *Theory of Electric Polarization, Vol. II, Dielectric in Time-Dependent Fields*, Elsevier, Amsterdam (1978).
[35] V.W. Couling, C. Graham. *Molec. Phys.*, **93**, 1 (1998).
[36] V.W. Couling, B.W. Halliburton, R.I. Keir, G.L.D. Ritchie. *J. Phys. Chem.* A, **105**, 4365 (2001).
[37] D.A. Kleinman. *Phys. Rev.*, **126**, 1977 (1972).
[38] I. Cacelli, A. Rizzo, C. Hättig. KORG, a program for the solution of the radial Schrödinger equation for bound, quasibound and continuum levels.
[39] A. Halkier, B. Kirchner, H. Huber, M. Jaszunski. *Chem. Phys.*, **253**, 183 (2000).
[40] B. Fernández, H. Koch. *J. Chem. Phys.*, **109**, 10255 (1998).
[41] I. Mills, T. Cvitaš, K. Homann, N. Kallay, K. Kuchitsu. *IUPAC, Physical Chemistry Division: Quantities, Units and Symbols in Physical Chemistry*, Blackwell Science, Oxford (1993).
[42] E.A. Donley, D.P. Shelton. *Chem. Phys. Lett.*, **215**, 156 (1993).
[43] E.A. Donley, D.P. Shelton. *Chem. Phys. Lett.*, **228**, 701 (1994).

Downloaded By: [Ruhr-universitaet Bochum] At: 14:21 3 November 2010